Progress in the Analysis and Design of Marine Structures – Guedes Soares & Garbatov (Eds)
© 2017 Taylor & Francis Group, London, ISBN 978-1-138-06907-7

Benchmark study on considering welding-induced distortion in structural stress analysis of thin-plate structures

I. Lillemäe-Avi & H. Remes
Marine Technology, Department of Mechanical Engineering, Aalto University, Finland

Y. Dong & Y. Garbatov
Centre for Marine Technology and Engineering (CENTEC), Instituto Superior Técnico, Universidade de Lisboa, Portugal

Y. Quéméner
CR Classification Society, Taiwan

L. Eggert
Lürssen Werft, Bremen-Vegesack, Germany

Q. Sheng & J. Yue
School of Transportation, Wuhan University of Technology, Wuhan, China

ABSTRACT: One of the key challenges for fatigue design of large welded thin structures is the consideration of initial distortions in the response analysis. The objective of this benchmark is to map the limitations of the current rules and to support the development of fatigue assessment guidelines for thin welded structures. The case study is a 4-mm thick full-scale stiffened panel, which is a part of a cruise ship deck structure and subjected to uniaxial uniformly distributed tensile load. The welding induced distortion related to butt-welded structure is included with different level of simplification and both shell and solid elements have been utilized in the finite element analysis. The estimated normal strain is compared with the experimentally measured one at a distance of approximately 8 mm away from the weld toe and root notches. The influence of modelling approach on the estimated structural hot spot stress and the fatigue critical location along the butt weld is compared and discussed.

1 INTRODUCTION

Wider utilization of thin plates ($t < 5$ mm) in marine structures is still very limited because of the uncertainties related to production, fatigue, buckling, and vibration issues. One of the main challenges for fatigue design is the welding-induced initial distortion and its consideration in the response analysis (Remes et al 2016).

Due to lower bending stiffness of thin plates, the welding-induced distortion is not only larger but also with different shape compared to thicker plates (Lillemäe et al 2012, Eggert et al 2012). Even if the magnitude of the distortion is reduced by applying low heat input production methods such as laser-hybrid welding, the structural stress is still very sensitive to the local curved shape that varies along the weld (Lillemäe et al 2012, 2016b, 2017). In addition, the distortion may decrease under the axial tensile loading, making the structural stress nonlinearly dependent on the shape of the plate, the constraint from the surrounding structure and the applied load level (Lillemäe et al 2012, 2013, 2016b). Traditional rule-based fatigue assessment methods developed for thicker plates, see e.g. DNV (2014) & Hobbacher (2009), do not consider the effect of curved shape and geometrical nonlinearity and therefore, cannot describe the fatigue strength of thin-plate structures properly. Careful consideration of the structure's initial shape is needed in order to, firstly, determine the required accuracy of the geometry modeling, and secondly, to establish the appropriate limits for the shape and magnitude of the distortion, corresponding to a certain fatigue capacity.

The objective of this benchmark is to map the limitations of the current rules and to support the development of fatigue assessment guidelines for thin welded structures. As a straightforward comparison with full-scale experiments (Lillemäe et al 2016b, 2017) is available, this study increases the understanding in fatigue behavior of thin welded structures, a topic that has so far been studied using mostly small-scale specimens (Lillemäe et al 2012, Fricke & Feltz 2013, Fricke et al 2015).

An accurate geometry model of a 4-mm thick full-scale panel specimen is provided to all participants, who introduce different levels of simplification to it. The estimated normal strain is compared with the experimentally measured one close to fatigue critical butt joint. The influence of modeling approach on the structural hot spot stress as well as on the fatigue critical location along the weld is compared and discussed. Finally, suggestions for the further development of fatigue assessment guideline for thin welded structures are given.

2 BENCHMARK DESCRIPTION

2.1 *Structure*

A 4-mm thick cruise ship deck panel used in this benchmark study is presented in Figure 1. It is made of normal structural steel with the yield strength of 320 MPa for the deck plating. The welding sequence was first the butt joint, then stiffeners and finally the web frames, see Figure 2. The full-scale test specimen cut from this panel was 3360 mm long and 540 mm wide, see Figure 3 and Figure 6. The spacing of stiffeners (HP80 × 5) and web frames (T440 × 7/150 × 10) was 404 and 2560 mm, respectively. These structural dimensions would be reasonable for cruise ship superstructure decks, considering also the restrictions from buckling and production cost.

The geometry measurements of the panel were carried out using optical system with two cameras and the minimum accuracy in lateral direction of 0.02 mm. The overall shape was measured only from the stiffeners side of the plate, whereas the fatigue critical laser-hybrid welded butt joint, located half way between the web frames, was measured from both sides. Benchmark participants were provided with the point cloud of the overall panel shape (Lillemäe et al 2017), Figure 3, as well as with the mean weld geometry of the butt joint, defined from the analysis of the small-scale specimens cut from the same panel, see Table 1. Contour plot of initial distortion is shown in Figure 4 and one longitudinal and 3 transverse sections cut from it are presented in Figure 5.

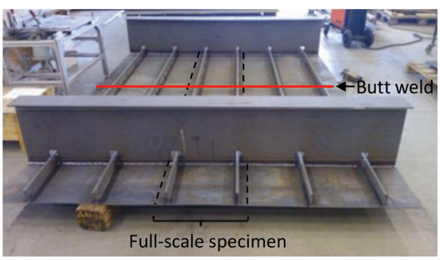

Figure 1. 4-mm thick cruise ship deck panel.

Figure 2. Welding of the stiffeners.

2.2 *Test setup*

The test specimen was attached to the test frame as shown in Figure 6. The test was force-controlled with the load ratio of R = 0.1. The minimum and maximum applied load was 62 and 620 kN, respectively, resulting in nominal stress range of 171 MPa. Force and strains at selected locations were recorded during the test. Special clamping system was used to apply force to the neutral axis of the panel and to proportionally transfer the load to deck plate and stiffeners. These boundary conditions represent realistic loading on the deck panel in cruise ship superstructure as shown in Lillemäe (2014). In the analysis, simplified boundary conditions may be applied to the location where the clamping plates ended, i.e. approximately 100 mm

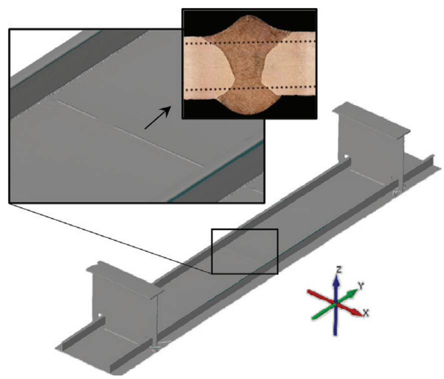

Figure 3. Geometry model visualized in Gom Inspect Free software.

Table 1. Mean weld geometry based on small-scale specimen analysis (Lillemäe et al 2016a).

	Toe		Root	
	Left	Right	Left	Right
Weld width, mm	5.4		4.3	
Weld height, mm	1.1		0.9	
Flank angle, deg	13	18	26	28
Radius, mm	1.26	1.05	0.79	0.62
Undercut, mm	0.047	0.027	0.011	0.013

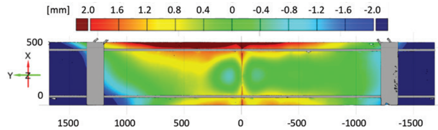

Figure 4. Initial distortion contour.

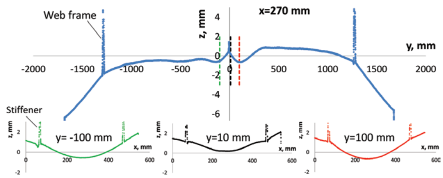

Figure 5. Initial distortion shape in longitudinal direction in the middle of the panel (x = 270 mm) and in transverse direction at y = −100, 10 and 100 mm.

Figure 6. Full-scale specimen in the test setup.

outside web frames. It can be assumed that one end of the panel was clamped and on the other end the force was applied with constant displacement.

2.3 *Methods*

Each benchmark participant was free to choose the approach for structural analysis, including the way of handling the geometry data. The participants were expected to report the fatigue critical location along the butt weld and the structural hot spot stress range in that location under the given applied load level. To validate the analysis, the normal strain at the strain gauge locations approximately 8 mm from each weld notch as well as the total displacement at the end of the panel was also required.

For structural hot spot stress analysis, two options were possible. First was the rule based nominal stress approach, where the provided geometry data is utilized to evaluate the most fatigue critical location and to extract the misalignments. The stress magnification factor due to axial misalignment can be determined as (Hobbacher, 2009):

$$k_{m\_axial} = 1 + \frac{3 \cdot e}{t} \tag{1}$$

where e = axial misalignment; and t = plate thickness. The stress magnification factor due to angular misalignment assuming fixed boundary conditions can be determined as (Hobbacher, 2009):

$$k_{m\_angular} = 1 + \frac{3 \cdot \alpha \cdot l}{2 \cdot t} \cdot \left[\frac{\tanh(\beta/2)}{\beta/2} \right] \tag{2}$$

where α = angular misalignment in radians; l = support length; and

$$\beta = \frac{2 \cdot l}{t} \cdot \sqrt{\frac{3 \cdot \sigma_{\max}}{E}} \tag{3}$$

where σ_{max} = maximum applied nominal stress; and E = Young's modulus.

When pinned boundary conditions are assumed, eq. (2) becomes:

$$k_{m\_angular} = 1 + \frac{3 \cdot \alpha \cdot l}{t} \cdot \left[\frac{\tanh(\beta)}{\beta} \right] \tag{4}$$

The part in square brackets in eq.-s 2 and 4 consider geometrical nonlinearity, i.e. the straightening effect, and according to Hobbacher (2009) it can be disregarded if conservative design approach is applied.

The total stress magnification factor is:

$$k_m = 1 + (k_{m\_axial} - 1) + (k_{m\_angular} - 1) \tag{5}$$

Structural hot spot stress can then be calculated by multiplying the k_m factor with the nominal stress, defined as the force divided by the cross-sectional area.

The second option is to utilize the Finite Element (FE) analysis and the linear extrapolation of maximum principal stress according to IIW (Hobbacher, 2009), DNV (DNV, 2014) or other existing rule or guideline. This is a common structural stress approach.

2.4 *Participants*

The approaches chosen by each participant are described in sections 2.4.1 to 2.4.5. Summary of geometry handling is given in Table 2 and FE-modeling approaches and used software in Table 3. In all cases, the web frames and stiffeners were assumed to be straight and the plate thickness constant t = 4 mm. Fillet welds of stiffeners and web frames were not considered. Material behavior in FE analysis was assumed to be linear elastic with Young's modulus of E = 206–211 GPa and Poisson ratio ν = 0.3.

Table 2. Summary of geometry handling.

Participant	Approach
#1	Points at every 10 mm extracted from original data and used as nodes
#2	6th order polynomial fit
#3	6th order polynomial fit (3rd order outside web-frames)
#4	Buckling shape using 6 points from original data + 4 points close to butt weld, simplified shape in transverse direction
#5	Quartic fit close to butt weld + quadratic elsewhere

Table 3. Summary of FE modeling and analysis approaches.

Participant	Approach
#1	4-node shell + 2D plane stress sub-model; Abaqus
#2	8-node solid (Solid185 with enhanced strain), Ansys
#3	4-node shell; Abaqus and NX Nastran
#4	4-node shell; Abaqus
#5	8-node solid; Ansys

2.4.1 *Participant #1*

Points at every 10 mm were extracted from the original geometry data and applied as nodal displacements on the straight panel FE model. After solving the model, the deformations were made permanent and stresses were zeroed. In order to guarantee high accuracy especially around the fatigue critical butt joint area, the resulting distortions were compared with the original data and manually corrected where necessary. The distorted stress-free structure was then used as an initial geometry for the axial tensile loading from the test setup. The model was created using four-node shell elements and the mesh size was 5 mm close to fatigue critical butt weld and 10 mm elsewhere. The weld profile was not modeled, but one row of elements coinciding with the butt weld had larger plate thickness to consider higher stiffness.

For calculating the hot spot stress the 2D plane stress sub-models with the mesh size varying from 0.1 mm in the notch to 0.8 mm at the boundaries were created at the fatigue critical area along the butt weld. The displacements from the geometrically nonlinear panel model were applied on the boundaries of the local linear models. The hot spot stress was defined using linear extrapolation of maximum principal stress according to IIW (Hobbacher, 2009), i.e. using points 0.4t and 1.0t from the fatigue critical notch. For both panel and local models Femap 11.0 was used for pre- and post-processing and Abaqus 6.13 for analysis. The FE-models and the analysis procedure are presented in Figure 7.

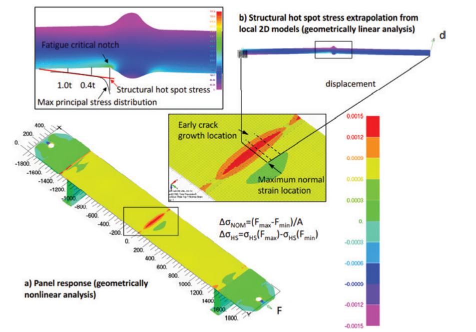

Figure 7. FE-model and analysis procedure of participant #1.

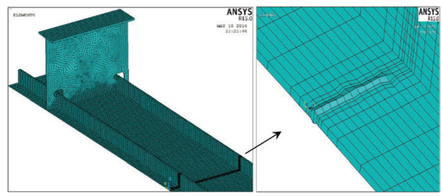

Figure 8. FE-model of participant #2.

2.4.2 *Participant #2*

The geometry of the panel was described with the 6th order polynomial regression equations fitted through the data in transverse direction with 5-mm steps in longitudinal direction. The least-square method was employed. The nodal locations of an ideally straight model were then shifted to correspond to the distorted shape. The FE-model was created using 8-node solid elements with linear shape functions and enhanced strain capabilities. The overall mesh size was $25 \times 5 \times t$. Close to fatigue critical butt weld the size decreased to enable hot spot stress extrapolation using nodes at 0.4t and 1.0t (Hobbacher, 2009) and at 0.5t and 1.5t from the weld notch (DNV, 2014). The weld profile was modeled using uneven thickness defined using 3 points as shown in Figure 8. The analysis was carried out with Ansys FE-software considering geometrical nonlinearity. In addition, axial and angular misalignments and the stress magnification factors according to IIW (Hobbacher, 2009) were determined along the butt weld.

2.4.3 *Participant #3*

The panel was divided into 6 parts in stiffener direction and polynomial regression equations were fitted on the 5-mm bandwidth of plating distortion data (x-direction), employing the least-square method. The polynomials were of 6th order, except for the panel ends outside web frames, where the 3rd order was used. The overall plate distortion was described using in total 636 polynomial equations. FE-model was created with four-node shell elements, see Figure 9. Overall mesh size was 20 mm and decreased close to butt weld to enable hot spot stress extrapolation according to IIW (0.4t and 1.0t; Hobbacher, 2009) and DNV (0.5t and 1.5t; DNV, 2014). The weld profile was not modeled, but the axial misalignment was included using rigid links that kinematically coupled the two parts of the panel. Analyses were carried out considering geometrical nonlinearity and using both Abaqus and NX Nastran FE-software.

In addition, the rule-based method was applied, where first a finer examination of plate distortions was conducted in the vicinity of fatigue critical butt joint to determine axial and angular misalignment. The stress magnification factors were defined according to IIW (Hobbacher, 2009) equations with and without considering the straightening effect. Sensitivity of a chosen support length *l* (eq.-s 2–4) on the final result was also studied and discussed.

2.4.4 *Participant #4*

The overall geometry of the plate field was defined with buckling shape using 6 equally spaced points in the longitudinal direction, taken from between the stiffener spacing. Additional 4 points (at 5 and 15 mm from both sides of the weld notch) were needed to define axial and angular misalignment and these were added to the model according to geometry idealization developed for 1200 × 400 mm plate fields presented by Eggert (2015), see Figure 10. Before picking the points, the original data had to be shifted and turned so that the web frame locations would be at a z = 0 level. In transverse direction a simplified half buckling wave shape was assumed, again so that the stiffener-plate intersection line would be at a z = 0 coordinate. As the points for defining the shape were taken from the middle of the plate between stiffeners, i.e. no variation in transverse direction was considered, then also the most fatigue critical location was at the middle of the plate.

The FE model was created using shell elements. The overall mesh size was 10 mm, but smaller close to butt weld to enable hot spot stress extrapolation

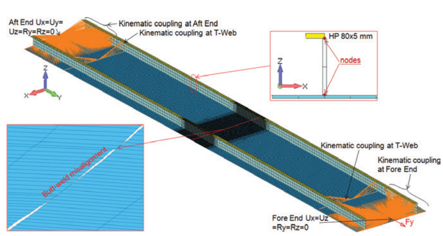

Figure 9. FE-model of participant #3.

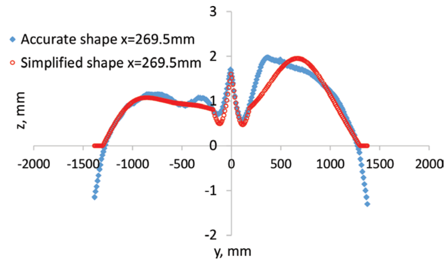

Figure 10. Simplified shape in the middle of the plate field between stiffeners.

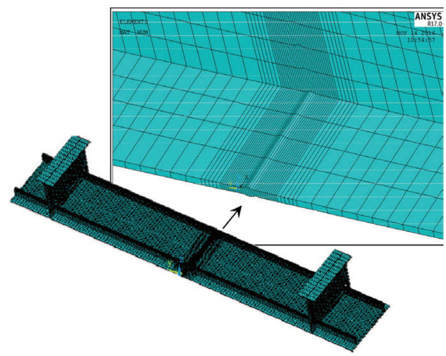

Figure 11. FE-model of participant #5.

according to IIW (Hobbacher, 2009), i.e. using points at 0.4t and 1.0t from the fatigue critical notch. The analysis was carried out geometrically linearly as well as nonlinearly.

2.4.5 *Participant #5*

Initial distortion shape was described using quadratic polynomial functions fitted through the data in transverse direction. Close to butt weld additional quartic fitting was performed. The minimum distance between the fitting points was 1 mm close to butt weld and 25 mm farther from it. FE-model was created using 8-node solid elements with the size of 10 × 0.25t × t close to butt weld and 10 × 25 × t elsewhere, see Figure 11. The analysis was carried out with Ansys FE-software considering geometrical nonlinearity. The hot spot stress range was defined using linear extrapolation according to DNV (2014).

3 RESULTS

The fatigue critical locations and corresponding hot spot stress ranges are presented in Table 4. The estimated fatigue critical location varied between x = 300 and 320 mm for participants #1–3 and 5 and was exactly in the middle of the panel at x = 270 mm for participant #4 because of the simplified shape

Table 4. Hot spot stress range ($\Delta\sigma_{HS}$) and stress magnification factor (k_m) at fatigue critical location defined using different approaches.

		Structural stress approach					
		Lin ext IIW		Lin ext DNV		Nominal stress approach	
	Fat crit. loc.	$\Delta\sigma_{HS}$	k_m[a]	$\Delta\sigma_{HS}$	k_m[a]	k_m (eq. 1–5)	$\Delta\sigma_{HS}$[b]
#1	y- /z- /x = 320	319	1.87				
#2	y- /z- /x = 305	313	1.83	306	1.79	2.69[c] (1.72[d])	460[c] (294[d])
#3	y- /z- /x = 300	326	1.91	314	1.84	2.40[c]	410[c]
#4	y- /z- /x = 270	304 (356[e])		1.78			
#5	y- /z- /x = 304.5			288	1.68		
exp. y- /z- /x =325							

[a] $k_m = \Delta\sigma_{HS}/\Delta\sigma_{NOM}$, $\Delta\sigma_{NOM}$ defined as $(F_{max}-F_{min})/A$, where A = 3260 mm².
[b] $\Delta\sigma_{HS} = k_m$ (eq. 1–5)$*\Delta\sigma_{NOM}$.
[c] Support length in eq. 2 assumed to be l = 60 mm. Straightening effect not included.
[d] l = 60 mm and straightening considered with eq. 4 (assuming pinned ends).
[e] Geometrically linear FE analysis.

in transverse direction. The observed primary crack initiation location was at x = 325 mm, but many secondary initiations were present in the area between x = 290…330 mm, see Figure 12.

The hot spot stress range varied between 304 and 326 MPa, defined using geometrically nonlinear FE analysis and linear extrapolation according to IIW (Hobbacher, 2009) at the most fatigue critical location. Linear extrapolation according to DNV (2014) with larger extrapolation distances gave slightly lower values, i.e. from 288 to 314 MPa. Geometrically linear FE analysis resulted in higher hot spot stress range, i.e. 356 MPa instead of 304 MPa for participant #4. Differences between two FE software employed by participant #3 were insignificant.

When hot spot stress range is defined using nominal stress range and equations 1–5 without considering the straightening effect, the values are significantly overestimated. When straightening is considered, the values are closer to the ones obtained using geometrically nonlinear FE analysis and linear extrapolation. However, it must be noted that both the stress magnification factor due to angular misalignment as well as the straightening depend on the chosen support length l. For large structures it is difficult to define the support length because of the curved shape.

The normal strain distribution at the fatigue critical side of the weld approximately 8 mm from the notch, where the strain gauges were located, is plotted in Figure 13. For participants #1–3 and 5 the strain distribution agrees well with the experiments, when geometrically nonlinear FE analysis is applied. Geometrically linear analysis overestimates the strains. The result of participant #4 agrees well with the experiments only in the middle of the specimen, where the geometry was most accurately modeled. Simplified shape in transverse direction causes inaccuracy.

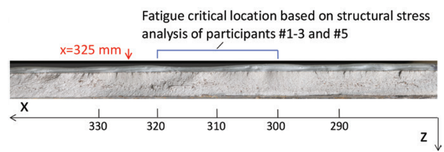

Figure 12. Fracture surface.

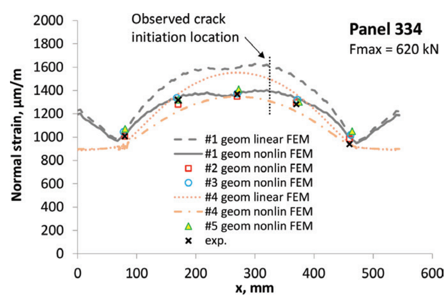

Figure 13. Normal strain distribution at the most fatigue critical side of the weld (y- & z-).

4 DISCUSSION

The level of geometry simplification was the highest for participant #4 who only used 6 + 4 points in longitudinal direction from the middle of the stiffener spacing to define the entire initially distorted panel shape. The second simplest was participant #5 who used quadratic equations to fit the original data. Close to butt weld additional quartic fit was applied to have a better match. Rest of the participants had more accurate models, where sorted raw data or the 6th order polynomial fitting was used.

When geometrically nonlinear FE-analysis is used, the results of all participants agree very well with the experiments. All results stayed within

10%, but most of them even within 5% from the experiments. Also the fatigue critical location along the butt weld was predicted with sufficient accuracy, considering the almost constant strain distribution in the area of approximately x = 300… 330 mm (Figure 13) and multiple crack initiation locations indicated in the fracture surface (Figure 12). The simplified shape of participant #4 was able to catch the correct strain in the middle of the panel and close to one stiffener, but was inaccurate elsewhere. Considering that the level of geometry simplification applied by participant #4 was much higher compared to others, the result is promising, but the approach should be further developed to account for varying shape in transverse direction by e.g. including few extra points. This is important in order to capture the correct fatigue critical location along the weld. Another interesting observation is that the strains predicted by participant #5 agree very well with the experiments and other results, but the hot spot stress defined in the fatigue critical location is lower than those of others.

When geometrically linear FE-analysis applied, the strains are noticeably overestimated. This is similar as explained in Lillemäe et al (2016b). When the rule-based stress magnification factor is used to calculate the structural stress, the result is even more severely overestimated. This is both due to the curved shape of thin welded plates as well as the geometrically nonlinear behavior, which was explained in case of small-scale specimens in Lillemäe et al (2012) and Fricke et al (2015). IIW (Hobbacher, 2009) guideline for fatigue assessment of welded joints and components includes the geometrically nonlinear straightening effect in their equation (see eq. 2 and 4), but they assume that the angular misalignment is formed between straight plates. As shown in Lillemäe et al (2012), the curved shape influences the straightening behavior significantly. Figure 14 illustrates how for a chosen support length of l = 60 mm the IIW (Hobbacher, 2009) analytical solution with straightening under- and without straightening overestimates the structural stress.

In addition, there is a problem of choosing the support length l in case of large structure with curved shape. The length l is used for determining the angular misalignment as well as for calculating the stress magnification caused by angular misalignment. It is also used in β equation, which defines the straightening. The sensitivity of the chosen support length l on the angular misalignment is presented in Figure 15. The angular misalignment in case of l = 20 mm is 1.85° and in case of l = 60 mm it is 1.64°. The effect of the chosen support length on the structural hot spot stress, when the straightening effect is included with eq.-s 2 and 4, can be seen in Figure 16 and Figure 17. As a coincidence, the pinned boundary conditions and the support length of l = 40 mm gave

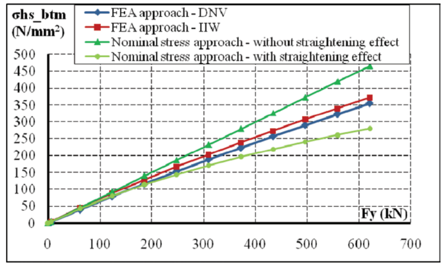

Figure 14. Influence of straightening on the structural stress compared to geometrically nonlinear FE-solution, l = 60 mm, pinned boundary conditions, x = 300 mm.

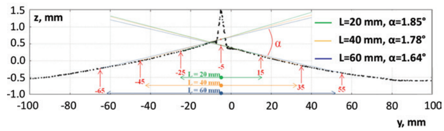

Figure 15. Sensitivity of angular misalignment on the chosen support length l.

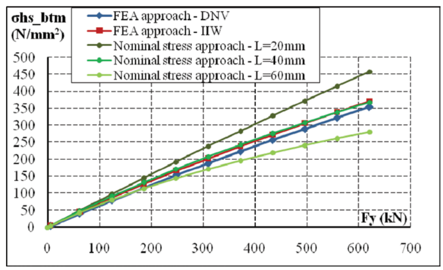

Figure 16. Sensitivity of structural stress (straightening included) on the chosen support length l in case of pinned boundary conditions; at x = 300 mm.

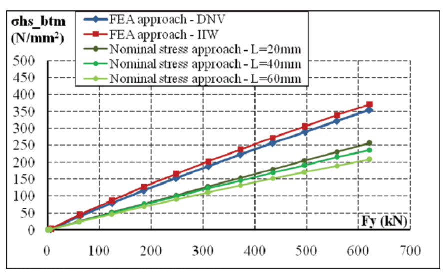

Figure 17. Sensitivity of structural stress (straightening included) on the chosen support length l in case of fixed boundary conditions; at x = 300 mm.

the best agreement with the geometrically nonlinear FE-solution, while l = 20 mm over- and l = 60 mm underestimated the stress. For fixed boundary conditions all support lengths underestimated the stress. However, this depends on the exact local curved shape and cannot be generalized without analyzing more panels with different shapes. In addition, one should notice that the support length of 20–60 mm is significantly smaller than the real physical support length, i.e. the web frame spacing (2650 mm) commonly applied for thick plates.

5 CONCLUSIONS

From the benchmark study on considering the welding-induced initial distortions in the structural stress analysis of thin-plate structures, following conclusions can be drawn:

- The structural stress is strongly influenced by the local curved shape and the geometrical nonlinearity. All participants who included the shape in both directions and used geometrically nonlinear analysis ended up with good agreement compared to experiments. Even the highest level of simplification where the distortion shape was only included in longitudinal direction gave very good results in the middle of the panel. If the transverse shape could be considered by adding few extra points, the approach might be enough to capture the structural stress accurately in the whole panel.
- Angular misalignment is sensitive to the location where it is defined because of the curved shape.
- Rule-based equation for stress magnification leads to significant overestimation of the structural stress when straightening effect is not included. If it is included, it can lead to over- or underestimated results as it is very sensitive to the chosen support length.

This study gave an insight to the required modeling accuracy, but for fatigue design of thin welded structures, a more comprehensive sensitivity analysis is needed to determine the limits for the distortion shape and magnitude to correspond to a certain fatigue capacity. Also, the IIW (Hobbacher, 2009) stress magnification and straightening equation could be studied further to see if it can be adjusted for curved shapes of large structures. Especially the definition of the support length for analytical equations requires additional considerations.

ACKNOWLEDGEMENTS

This paper is a result of a joint effort of International Ship and Offshore Structures Congress (ISSC) 2018 Fatigue & Fracture III.2 committee. The full-scale experiments used as validation in this work were carried out in Aalto University within the Future Digital Manufacturing Technologies project (MANU) of Finnish Metals and Engineering Competence Center (FIMECC). The full-scale structures were manufactured in cooperation with Meyer Turku shipyard and Winnova Oy.

REFERENCES

Det Norske Veritas. 2014. Fatigue Assessment of Ship Structures, Classification Notes 30.7.

Eggert, L., Fricke, W., Paetzhold, H. 2012. Fatigue strength of thin-plated block joints with typical shipbuilding imperfections. *Welding in the World* 56 (11-12): 119–128.

Eggert, L. 2015. Betriebsfestigkeit von Dünnblech-Montagestößen mit werftüblichen Imperfektionen im Schiffbau. Doctoral Dissertation. Hamburg University of Technology, Hamburg, Germany.

Fricke, W., Feltz, O. 2013. Consideration of influence factors between small-scale specimens and large components on the fatigue strength of thin-plated block joints in shipbuilding. *Fatigue & Fracture of Engineering Materials & Structures* 36 (12): 1223–1231.

Fricke, W., Remes, H., Feltz, O., Lillemäe, I., Tchuindjang, D., Reinert, T., Nevierov, A., Sichermann, W., Brinkmann, M., Kontkanen, T., Bohlmann, B., Molter, L. 2015. Fatigue strength of laser-welded thin-plate ship structures based on nominal and structural hot-spot stress approach. *Ships and Offshore Structures* 10 (1): 39–44.

Hobbacher, A. 2009. Recommendations for Fatigue Design of Welded Joints and Components, IIW doc. 1823-07, Welding Research Council Bulletin 520, New York.

Lillemäe, I., Lammi, H., Molter, L., Remes, H. 2012. Fatigue strength of welded butt joints in thin and slender specimens. *International Journal of Fatigue* 44: 98–106.

Lillemäe, I., Liinalampi, S., Remes, H., Avi, E., Romanoff, J. 2016b. Influence of welding distortion on the structural stress in thin deck panels. PRADS 2016, 4–8 September 2016, Copenhagen, Denmark.

Lillemäe, I., Liinalampi, S., Remes, H., Itävuo, A., Niemelä, A. 2017. Fatigue strength of thin laser-hybrid welded full-scale deck structure. *International Journal of Fatigue* 95: 282–292.

Lillemäe, I., Remes, H., Liinalampi, S., Itävuo, A. 2016a. Influence of weld quality on the fatigue strength of thin normal and high strength steel butt joints. *Welding in the World* 60 (4): 731–740.

Lillemäe, I., Remes, H., Romanoff, J. 2013. Influence of initial distortion on the structural stress in 3 mm thick stiffened panels. *Thin-Walled Structures* 72: 121–127.

Lillemäe, I., Remes, H., Romanoff, J. 2014. Influence of initial distortion of 3 mm thin superstructure decks on hull girder response for fatigue assessment. *Marine Structures* 37: 203–218.

Remes, H; Romanoff, J; Lillemäe, I; Frank, D; Liinalampi, S; Lehto, P; Varsta P. Factors affecting the fatigue strength of thin-plates in large structures. *International Journal of Fatigue*, Available online 15 November 2016.